ISSN 2176-5480

22nd International Congress of Mechanical Engineering (COBEM 2013)
November 3-7, 2013, Ribeirão Preto, SP, Brazil

INFLUENCE OF TEMPERATURE VARIATIONS ON THE VIBRATION OF SHAPE MEMORY ALLOY STRUCTURES USING FINITE ELEMENT ANALYSIS

Klaus Reis von H. Lima
Marcelo A. Savi
Department of Mechanical Engineering, Universidade Federal do Rio de Janeiro, Rio de Janeiro, RJ 21.941.972, Brazil
klauslima89@poli.ufrj.br, savi@mecanica.ufrj.br

Darren J. Hartl
Dimitris C. Lagoudas
Department of Aerospace Engineering, Texas A&M University, College Station, TX 77843, USA
darren.hartl@tamu.edu, lagoudas@tamu.edu

Abstract. *Structures with active materials such as shape memory alloys (SMAs) are of special interest for aerospace and mechanical applications. This paper employs the finite element method for analyzing the dynamics of SMA structures. Archetypal models are employed using the Hartl-Lagoudas SMA constitutive model and truss element type. The analyses are performed using the ABAQUS/Standard implicit finite element solver. Thermal loads are analyzed and the influence of the SMA thermomechanical coupling is observed. Initially, a structure of four SMA wires in two perpendicular directions connected to a central mass is considered. Each SMA wire is connected to a rigid base structure, which is submitted to forced vibration. A larger structure consisting of twelve wires interconnecting four masses undergoing free vibration is also considered. Temperature changes are imposed with the purpose of vibration control. It is shown that the finite element method is an effective tool for the dynamical analysis of smart structures, presenting good flexibility. The temperature dependent behavior of such structures indicates the adaptability that can be employed for vibration control purposes.*

Keywords: *Shape memory alloys, dynamics, vibration, finite element analysis, active materials*

1. INTRODUCTION

Shape Memory Alloys (SMAs) are metallic alloys that have unique characteristics due to its thermomechanical coupling. Under specific temperature and/or stress changes, these metals undergo solid-to-solid non-diffusive phase transformations. These transformations are responsible for interesting behaviors such as pseudoelastic and shape memory effects, which have held interest in several engineering applications.

Many authors have explored the nonlinear behavior of SMAs in order to alter the response of dynamical systems. A reason for this amount of interest is the great potential for applications in vibration control, as well as the possibility of observing interesting behaviors. In terms of applied dynamics, several applications have been studied exploring the adaptive dissipation associated with hysteresis loop of SMAs, and mechanical property changes due to phase transformations. In order to explore its particularities, SMA systems with few degrees-of-freedom have been widely discussed in the literature. Machado (2007) demonstrated how the intrinsic nonlinear characteristics of SMAs could affect the vibration of a one degree-of-freedom system by considering different accelerations and loading histories.

Some contributions have explored the possibility to reduce vibration by changing the stiffness of an SMA element with temperature variations. Williams *et al.* (2002) and Savi *et al.* (2011) made use of such idea adressing adaptive vibration absorbers incorporating SMA as a tuning element. Aguiar *et al.* (2012) have considered one and two degree-of-freedom SMA oscillators, analyzing by experimental point of view the influence of temperature variations on stiffness and hysteresis and how those affect the system's resonant conditions. Silva (2011) has focused on vibration control of a rotor-bearing system, comparing different temperatures behaviors.

In general, the nonlinear dynamics of SMA systems are very rich, being related to complex responses. The interesting behaviors of SMA oscillators have been discussed by different perspectives (Bernardini and Rega, 2005; Machado *et al.* 2009; Savi and Braga, 1993; Savi and Pacheco, 2004). Lacarbonara *et al.* (2004) have numerically investigated the nonlinear response of a one degree-of-freedom SMA oscillator, showing how a rich class of solutions, such as quasiperiodicity and chaos could arise in nearly adiabatic conditions. Bernardini and Rega (2007) focused on the characterization of the chaotic response of the pseudoelastic oscillator. Sitnikova *et al.* (2011) have analyzed an impact oscillator with SMA constraint, also achieving complex dynamics noticing the capabilities for vibration reduction with amplitude variations. The dynamical response of structures involving SMAs have also been the objective of research efforts. Savi and Nogueira (2010) investigated numerical simulations of the dynamics of a pseudoelastic two-bar truss, achieving complex behaviors.

Despite the several existing applications in the aerospace industry, there is still a demand for the understanding of large-

ISSN 2176-5480

scale structures (such as antennas) using SMA components. In this regard, SMA grids composed of masses connected by SMA actuators are of special interest. A mass connected to four SMA wire grid has been previously addressed by de Paula *et al.* (2012). This archetypal model allows one to understand the dynamical behavior of larger systems, which might contain hundreds of connected nodes. The approach was focused on the nonlinear nature of the dynamical response, giving special attention to bifurcations and chaotic attractors.

The use of finite element analysis (FEA) is important since it furnished flexibility on system analysis, allowing the understanding of complex phenomena as non-homogeneous behavior. The FEA implementation of SMA constitutive models has shown extremely effective as an alternative approach to problems presenting geometrical nonlinearities and the need for design optimization (Auricchio and Taylor, 1997; La Cava *et al.*, 2004; Bandeira *et al.*, 2006, Hartl *et al.*, 2011).

The SMA grid discussed in de Paula *et al.* (2012) was revisited in Peraza *et al.* (2013) using FEA. The authors studied the influence of the consitutive model, element type and structural configuration (all wires with same or different pre-strain) on response. It was observed how the element types and strucural configurations can affect the computational time and the nonlinearity of the response, respectively.

This contribution deals with the vibration analysis of SMA grids employing the FEA. Two different structures are investigated. Initially, an SMA grid with one mass connected with four SMA actuators is treated. Afterward, a structure with twelve wires interconnecting four masses is analyzed in free response. Vibration control with temperature variations is studied in different configurations.

2. SHAPE MEMORY ALLOY CONSTITUTIVE MODEL

The thermomechanical behavior of SMAs may be described by constitutive models that establish a phenomenological description of these alloys. Lagoudas (2008) and Paiva and Savi (2006) presented a general overview about constitutive equations for SMAs. Here, the Hartl-Lagoudas model is employed considering the generation and recovery of transformation strains that occur as a result of martensitic transformation. Therefore, martensitic reorientation is not considered. The model considers three total external state variables: the stress $\boldsymbol{\sigma}$, the total strain $\boldsymbol{\varepsilon}$, and the absolute temperature T. Two internal state variables are also considered: the inelastic transformation strain $\boldsymbol{\varepsilon}^t$ and the martensitic volume fraction ξ. The temperature and the total strain are assumed to be the driving forces and therefore, are known. Additive decomposition is assumed by considering thermoelastic and inelastic contributions.

$$\boldsymbol{\varepsilon} = \boldsymbol{\varepsilon}^e + \boldsymbol{\varepsilon}^{in} = \boldsymbol{\mathcal{S}}(\xi)\boldsymbol{\sigma} + \boldsymbol{\alpha}(T - T_0) + \boldsymbol{\varepsilon}^t, \tag{2.1}$$

$\boldsymbol{\mathcal{S}}(\xi)$ is the phase-dependent fourth-order *compliance tensor*, written as

$$\boldsymbol{\mathcal{S}}(\xi) = \boldsymbol{\mathcal{S}}^A - \xi(\boldsymbol{\mathcal{S}}^A - \boldsymbol{\mathcal{S}}^M) = \boldsymbol{\mathcal{S}}^A - \xi\Delta\boldsymbol{\mathcal{S}}. \tag{2.2}$$

where $\boldsymbol{\mathcal{S}}^A$ and $\boldsymbol{\mathcal{S}}^M$ are the compliance tensors for austenitic and martensitic phases, respectively; $\boldsymbol{\alpha}$ is the second-order *coefficient of thermal expansion tensor*, where T_0 is the material reference temperature. Standard isotropic forms are assumed for $\boldsymbol{\mathcal{S}}(\xi)$ and $\boldsymbol{\alpha}$, and they are computed from material properties to be described shortly. The inelastic transformation strain evolves such that the time rate of change of both its magnitude and direction are given as

$$\dot{\boldsymbol{\varepsilon}}^t = \dot{\xi}\boldsymbol{\Lambda}^t = \dot{\xi}\begin{cases} H^{cur}(\bar{\sigma})\dfrac{3}{2}\dfrac{\boldsymbol{\sigma}'}{\bar{\sigma}} & ; \quad \dot{\xi} > 0 \\ \dfrac{\boldsymbol{\varepsilon}^{t-r}}{\xi^r} & ; \quad \dot{\xi} < 0 \end{cases}. \tag{2.3}$$

During forward transformation ($\dot{\xi} > 0$), the formulation for the direction of transformation follows the assumptions of classical associative Mises plasticity. The *Mises equivalent stress* is given as $\bar{\sigma} = \sqrt{(3/2\,\boldsymbol{\sigma}' : \boldsymbol{\sigma}')}$, where $\boldsymbol{\sigma}'$ is the deviatoric stress. The magnitude of transformation strain generated during full forward transformation is captured by the scalar-valued function $H^{cur}(\bar{\sigma})$. For trained materials, H^{cur} may be considered as follows:

$$H^{cur}(\bar{\sigma}) = \begin{cases} H_{\min} & ; \quad \bar{\sigma} \leq \bar{\sigma}_{crit} \\ H_{\min} + (H_{\max} - H_{\min})(1 - e^{-k(\bar{\sigma} - \bar{\sigma}_{crit})}) & ; \quad \bar{\sigma} > \bar{\sigma}_{crit} \end{cases}, \tag{2.4}$$

here $H_{\min}$, $H_{\max}$, k and $\bar{\sigma}_{crit}$ are model parameters.

During reverse transformation ($\dot{\xi} < 0$), the direction and magnitudes are defined such that all transformation strain existing at the cessation of forward transformation (i.e., at which time $\xi^r \leftarrow \xi$ and $\boldsymbol{\varepsilon}^{t-r} \leftarrow \boldsymbol{\varepsilon}^t$) is fully recovered should the material transform fully back into austenite. Having related stress, total strain, and inelastic strain, and further having defined an evolution equation for the inelastic strain $\boldsymbol{\varepsilon}^t$, we need only define constraints on the evolution of the martensitic volume fraction ξ, which acts as a scalar multiplier in (23). For this purpose, we introduce the transformation function $\Phi^t(\boldsymbol{\sigma}, T, \xi)$. Inspired by the methods of classical plasticity, we write constraints on evolution as

$$\Phi^t \leq 0, \quad \dot{\xi}\Phi^t = 0, \quad 0 \leq \xi \leq 1, \tag{2.5}$$

ISSN 2176-5480

where the first two represent the the Kuhn-Tucker constraints, and the third bounds the martensitic volume fraction, which ranges from 0 (pure austenite) to 1 (pure martensite).

Because forward and reverse transformation are distinctive processes (see (23), for example), and to ensure positive dissipation during both, we propose a branched form of Φ^t, given as

$$\Phi^t = \begin{cases} \Phi^t_{fwd}; & \dot{\xi} \geq 0 \text{ and } 0 \leq \xi < 1 \\ \Phi^t_{rev}; & \dot{\xi} \leq 0 \text{ and } 0 < \xi \leq 1 \end{cases} . \tag{26}$$

These two branches are given by

$$\begin{aligned} \Phi^t_{fwd} = \quad & (1-D)H^{cur}(\bar{\sigma})\bar{\sigma} - \tfrac{1}{2}\boldsymbol{\sigma} : \Delta\boldsymbol{\mathcal{S}}\boldsymbol{\sigma} - \rho\Delta s_0 T + \rho\Delta u_0 \\ & - \left[\tfrac{1}{2}a_1\left(1 + \xi^{n_1} + (1-\xi)^{n_2}\right) + a_3\right] - Y_0^t \end{aligned} , \tag{27}$$

$$\begin{aligned} \Phi^t_{rev} = \quad & -(1+D)\frac{\boldsymbol{\sigma} : \boldsymbol{\varepsilon}^{t-r}}{\xi^r} + \tfrac{1}{2}\boldsymbol{\sigma} : \Delta\boldsymbol{\mathcal{S}}\boldsymbol{\sigma} + \rho\Delta s_0 T - \rho\Delta u_0 \\ & + \left[\tfrac{1}{2}a_2\left(1 + \xi^{n_3} + (1-\xi)^{n_4}\right) - a_3\right] - Y_0^t \end{aligned} . \tag{28}$$

where D and Y_0^t are transformation dissipation parameters; $\rho\Delta s_0$ and $\rho\Delta u_0$ are the volume-specific change in reference to entropy and to internal energy between martensite and austenite, respectively; a_1, a_2, a_3 are transformation hardening coefficients while n_1, n_2, n_3, n_4 are transformation hardening exponents.

Model parameters for typical SMA is presented in Tab. 1. Numerical simulations can be performed using proper algorithm presented in Lagoudas (2008). The temperature dependent behavior of SMAs is illustrated by considering a wire subjected to a quasi-static mechanical loading path at different temperatures. Considering 300K as the reference temperature, it can be seen in Fig. 1 how the hysteretic loop goes to higher stress levels as the temperature increases, while the opposite occurs when the temperature decreases.

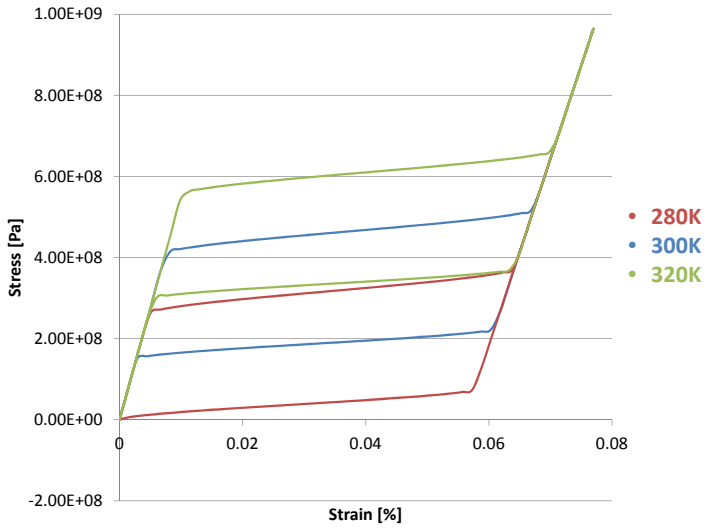

Figure 1. Isothermal loading response for three different temperatures (280K, 300K and 320K).

3. PHYSICAL STRUCTURES AND FEM

Large-scale structures can be modeled as multi degree-of-freedom systems. Aerospace applications include several structures, such as antennas, that can be represented by archetypal models defined from nodes connected with SMA elements. In this regard, two systems are investigated in this paper. The first one is composed of four wires interconnecting one centered mass to a rigid structure. The other system has twelve wires interconnecting four masses to a rigid structure. Figure 2 and Figure 3 present schematic sketches of both strutures.

Each wire has the length of 1m and circular cross section area of 1mm^2. Model parameters are the ones presented in Tab. 1. All of the wires are pre-tensioned to 3.8% strain (in the reference temperature of 300K) so they have initial martensitic volume fraction of 50% . The effects of gravity are neglected and the masses of 1kg are taken to be infinitesimally small, which means the absence of any rotational inertia. Additionally, only vertical excitation is considered.

ISSN 2176-5480

Table 1. Constitutive material properties associated with the Hartl-Lagoudas SMA model.

Material Properties	Values
E^A, E^M(GPa)	55, 46
$\nu^A = \nu^M$	0.33
M_s, M_f (K)	245, 230
A_s, A_f (K)	270, 280
C^A=C^M (MPa/K)	7.4
H	0.056
n_i (i=1,2,3,4)	0.5
ρ (kg/m^3)	6450

(a) Single-mass (b) Multi-mass

Figure 2. Studied structures

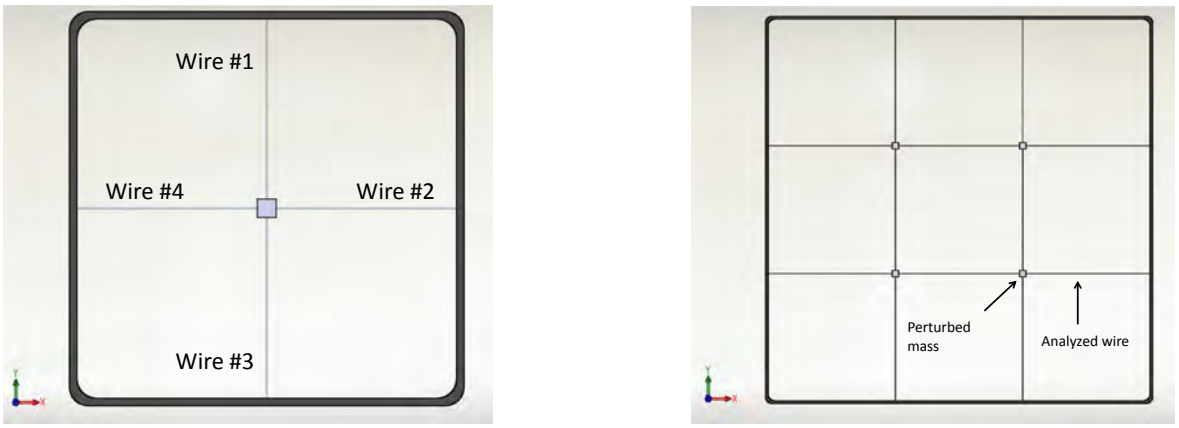

(a) Single-mass (b) Multi-mass

Figure 3. Structures references

The finite element method is employed to study the dynamical response of the two SMA structures. The analyses are performed using the ABAQUS/Standard implicit finite element solver, with Hartl-Lagoudas constitutive model. The SMA model is implemented through a user material subroutine (UMAT) (Lagoudas *et al.*, 2012).

The horizontal wires are aligned with the x axis, while the vertical wires are aligned with de y axis. Three-node quadratic truss elements are employed for spatial discretization. The FEA models are presented in Fig. 4. A point-mass of 1kg is assigned to every intersection of wires. Different analyses are of concern. Initially, the single-mass system is subject to forced vibrations. The multi-mass system is then analyzed in free response. Temperature changes are imposed to study vibration control capabilities.

ISSN 2176-5480

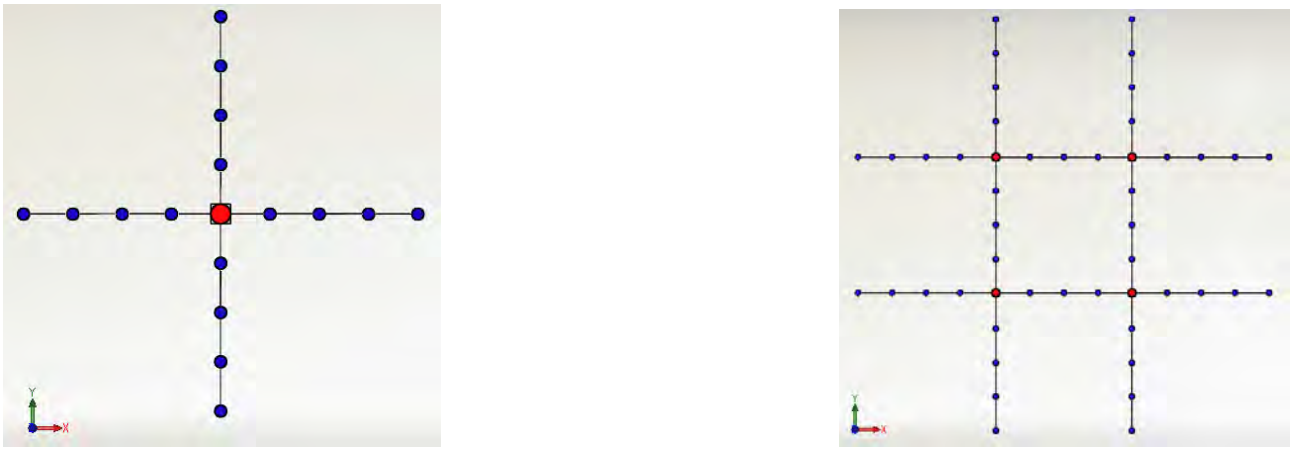

(a) Single-mass (b) Multi-mass

Figure 4. FEA models

4. NUMERICAL SIMULATIONS - SINGLE-MASS STRUCTURE

The influence of temperature variation on nonlinear dynamical response of SMA single-mass structure is now in focus. The main goal is to achieve lower amplitudes of response with temperature variations. An ideal case is considered where all the wires undergo the exact same temperature variations. A more realistic case, with non-homogeneous temperature is also considered. This is performed by keeping the wires #1 and #4 at constant temperature, while the #2 and #3 wires (Fig. 3a) are subjected to thermal loads. Since the hysteresis loop position at the stress-strain space can be controlled by temperature variations, it is possible to adjust hysteretic dissipation for control purposes.

Table 2. Symbols used in results.

Symbol	Physical values
SDV2 or ξ	Martensitic volume fraction
S.S11	Uniaxial Stress
U1,U2,U3	x,y,z displacements
V1,V2,V3	x,y,z velocities

4.1 Homogeneous temperature

This section treats the SMA structure with homogeneous temperature, which means that all wires are at the same temperature. Initially, consider that the structure is subjected to an external harmonic excitation in the vertical direction with a constant frequency of 55Hz, and different excitation amplitudes: 5g and 30g. All wires are subjected to the temperature variation (300K $\rightarrow$ 280K) with a rate of temperature change of 5K/s.

Figure 5 presents system response for external excitation of 5g, showing displacement time history and martensitic volume fractions. Note that temperature decrease promotes a vibration amplitude reduction due to phase transformation. Figure 6 shows the same behavior for an excitation amplitude of 30g. For both situations it is possible to identify the change of the equilibrium point position where the system oscillates.

4.2 Non-homogeneous temperatures

Non-homogeneous temperature behavior of the single-mass structure is focused on. Basically, wires #1 and #4 have constant temperature while wires #2 and #3 are subjected to temprature variations. For the excitation of 5g (Fig. 7) the response is dramatically different from the homogeneous case. When the excitation is 30g (Fig. 8) similar results are obtained. Note that for both situations, phase transformations are almost complete. For the case with 5g, volume fractions assume values greater than 0.8. When excitation is 30g, volume fractions are close to 1. This is associated with larger dissipation process due to hysteresis.

ISSN 2176-5480

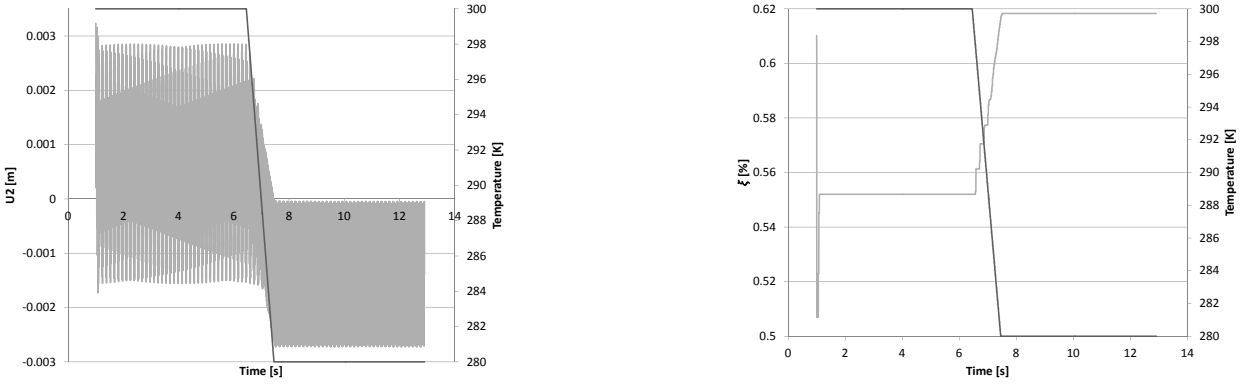

(a) Mass displacement (b) Martensitic volume fraction (down wire)

Figure 5. System response with homogeneous temperature and excitation of 5g with thermal load (300K $\rightarrow$ 280K)

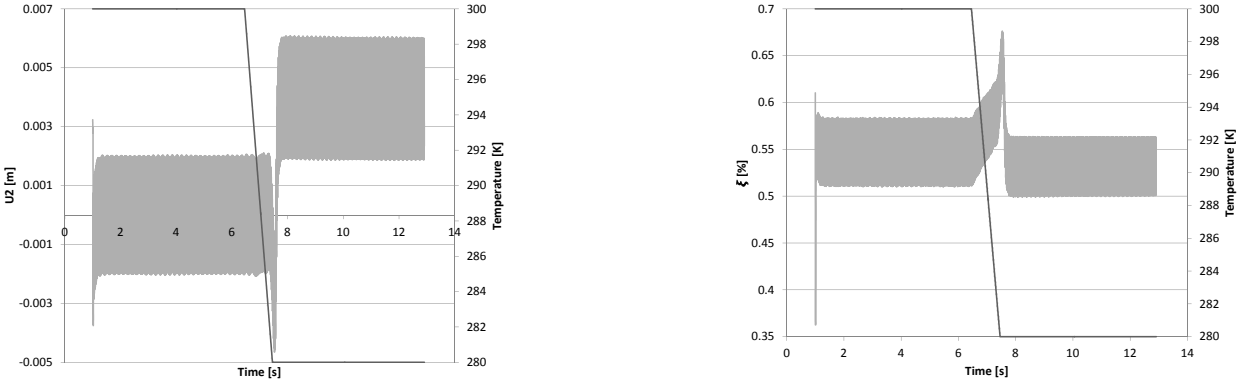

(a) Mass displacement (b) Martensitic volume fraction (down wire)

Figure 6. System response with homogeneous temperature and excitation of 30g with thermal load (300K $\rightarrow$ 280K)

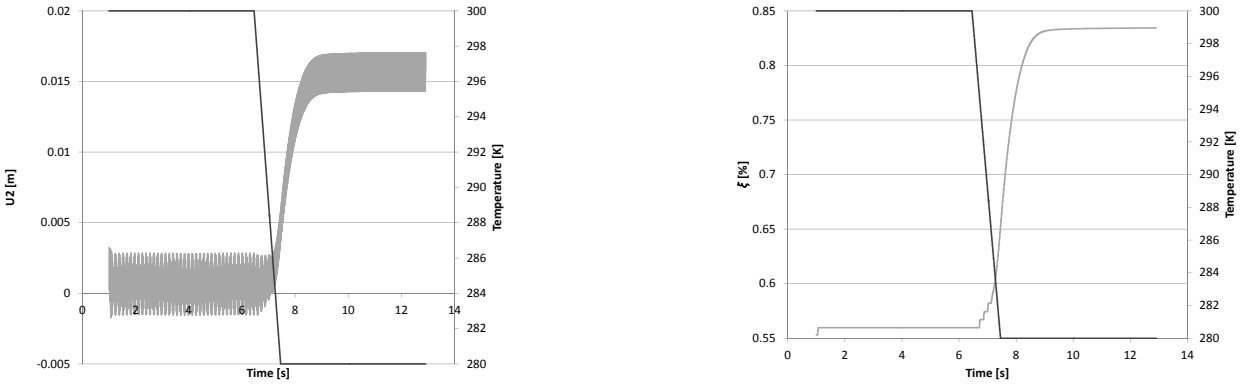

(a) Mass displacement (b) Martensitic volume fraction (down wire)

Figure 7. System response with non-homogeneous temperature and excitation of 5g, wires #2 and #3 with temperature change (300K $\rightarrow$ 280K), while wires #1 and #4 are at 300K.

5. NUMERICAL SIMULATIONS - MULTI-MASS STRUCTURE

The multi-mass structure is now analyzed. This extended version consists of a twelve wire structure interconnecting four masses, shown in Fig. 2b. In this case, only free response is taken into consideration, assuming out-of-plane motions. All wires have the same pre-strain and initial temperature of 250K (martensitic phase). One of the masses is perturbed and, during free response, thermal variations are imposed with the goal of vibration control. Initially, isothermal free response is treated. Afterward, all the twelve wires are heated from 250K to 400K, then cooled back to 250K. The displacements

ISSN 2176-5480

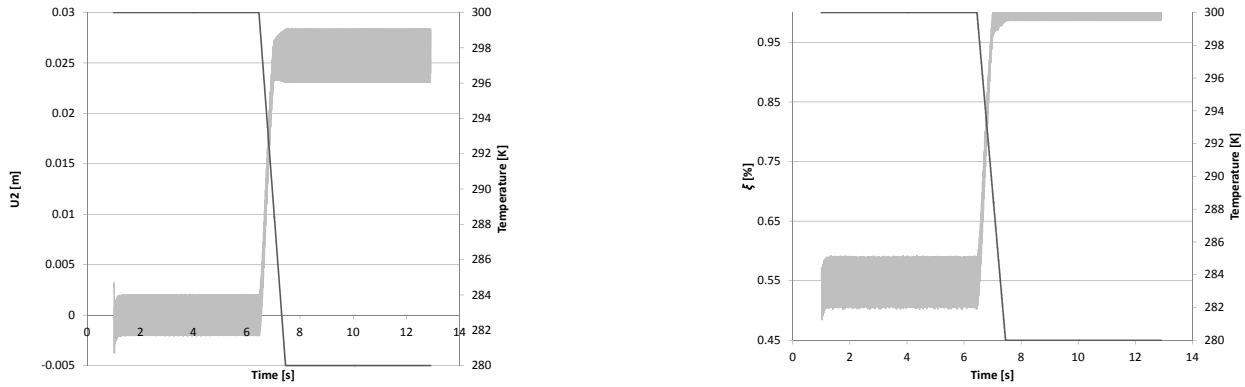

(a) Mass displacement

(b) Martensitic volume fraction (down wire)

Figure 8. System response with non-homogeneous temperature and excitation of 30g, wires #2 and #3 with temperature change (300K $\rightarrow$ 280K), while wires #1 and #4 are at 300K.

are all relative to the perturbed mass, while the stresses and martensitic volume fractions are all relative to the pointed wire, as previously exposed by Fig. 3b.

5.1 Constant temperature

This section considers constant temperature behavior of the multi-mass strucure. In Fig. 9, it is possible to see how the martensitic volume fraction remains constant. Therefore, elastic vibration occurs without any kind of dissipation. Figures 10 and 11 show the stress behavior on the chosen wire and the displacements in the three directions of the perturbed mass (U1, U2 and U3). It is noticeable how the on-plane displacements are similar (U1 and U2), while the out-of-plane vibration has higher amplitude and more interesting characteristics.

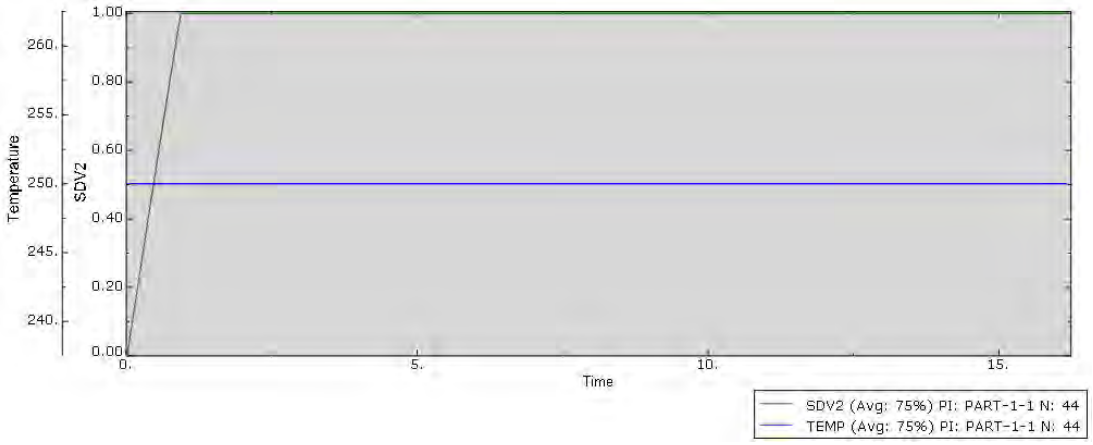

Figure 9. Martensitic volume fraction on the pointed wire

ISSN 2176-5480

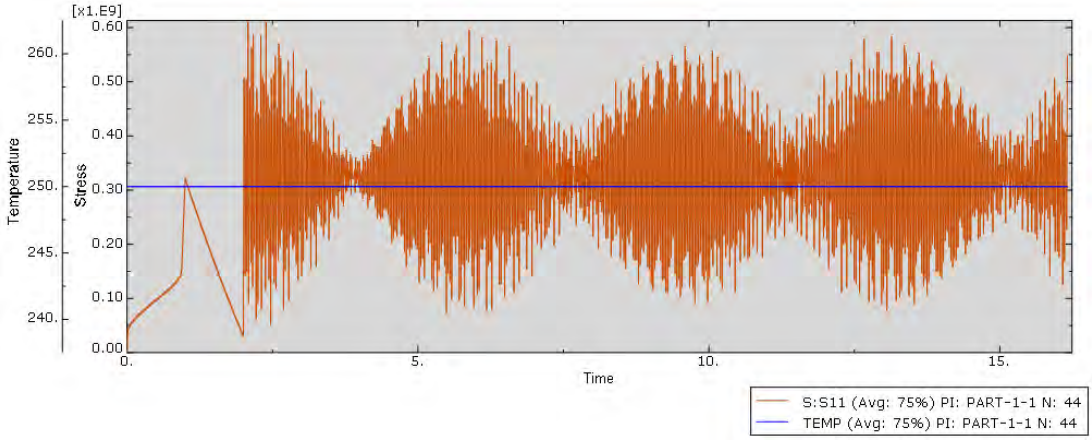

Figure 10. Stress on the pointed wire

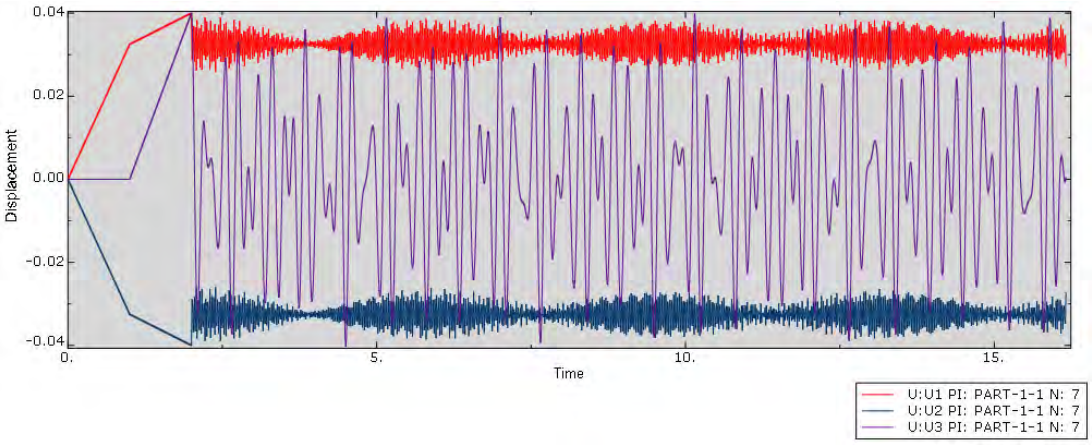

Figure 11. Perturbed mass displacement

ISSN 2176-5480

5.2 Temperature variations

This section considers situations with homeogeneous temperature variations. Figure 12 presents the system response showing how the temperature variation induces forward and reverse phase transformations, as the martensitic volume fraction (SDV2) changes. Furthermore, when the temperature increases to 400K, there is also an increase on the stress level (S.S11), which is related to the change in stiffness with phase transformation. The opposite occurs when the temperature comes back to 250K, though the stress amplitude is significantly reduced.

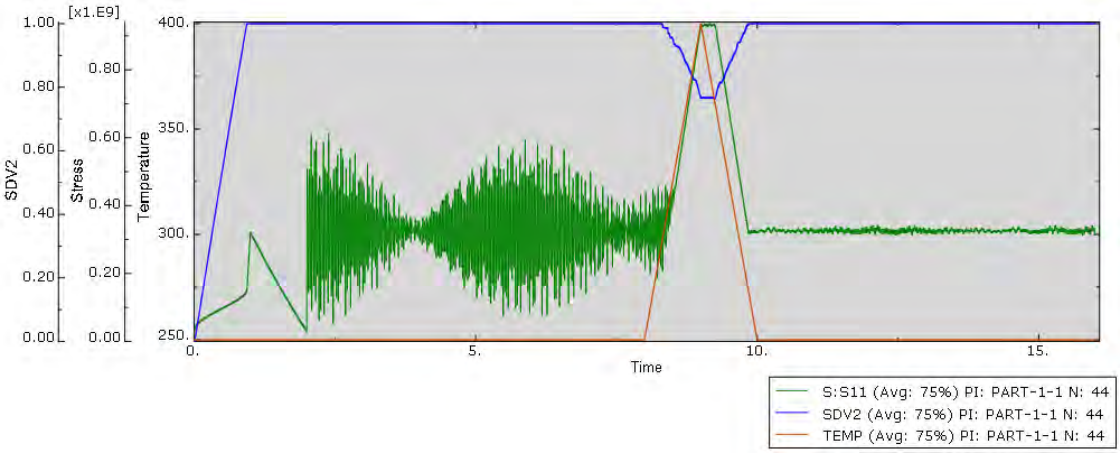

Figure 12. Martensitic volume fraction and stress on the pointed wire

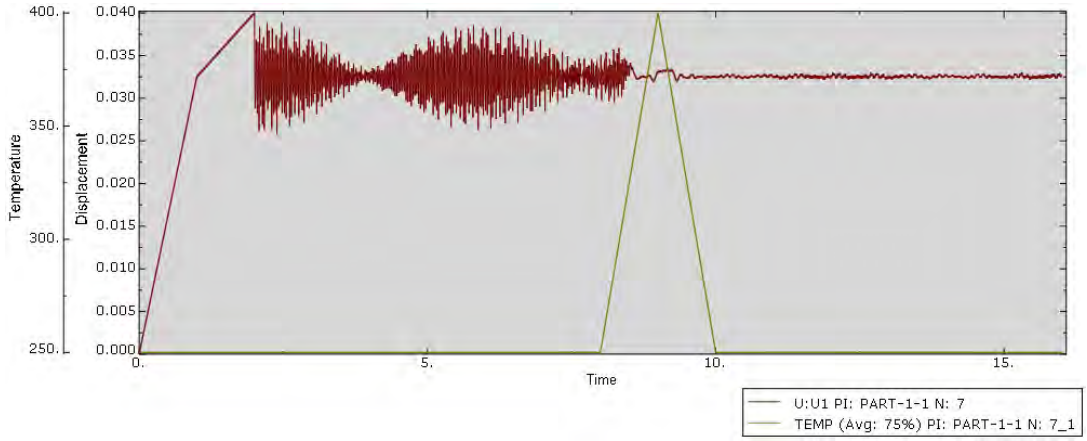

Figure 13. On-plane displacement (x direction)

The temperature change affects the on-plane motion the same way. The vibration amplitude on the x direction is presented in Fig. 13, which is reduced after the temperature variation. Figure 14 presents response for the out-of-plane motion, showing that the vibration reduction is not significantly observed in this situation.

6. CONCLUSIONS

In this work, a pseudoelastic SMA grid is analyzed using FEA. Two different archetypal models are treated: single-mass and multi-mass strucures. Temperature variations are imposed to both systems for different harmonic excitation amplitudes. Results show that it is possible to control the system response by using temperature variations. Either stiffness variations or dissipation effect can be exploited with this aim. Further effort will be dedicated to behaviors at different excitation frequencies.

Acknowledgments

The authors would like to acknowledge the support of the Brazilian Research Agencies CNPq, CAPES and FAPERJ and through the INCT-EIE (National Institute of Science and Technology - Smart Structures in Engineering) the CNPq and FAPEMIG. The Air Force Office of Scientific Research (AFOSR) is also acknowledged.

ISSN 2176-5480

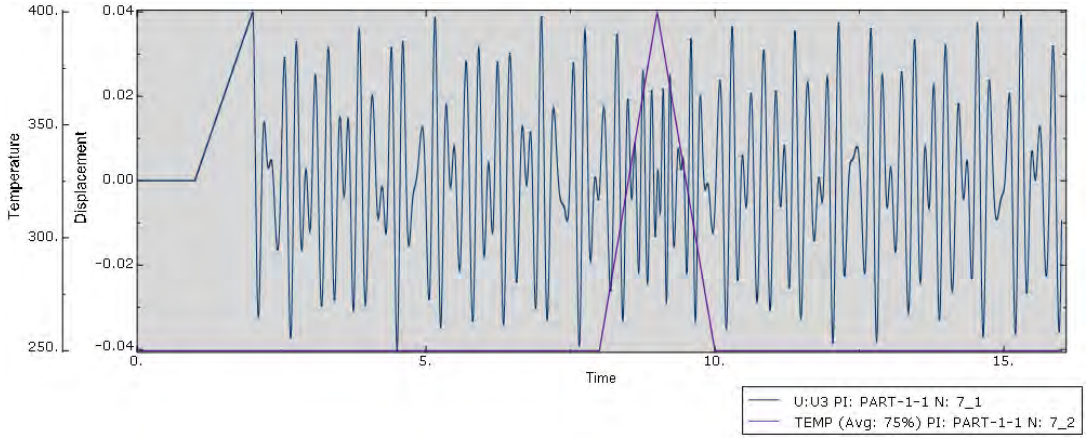

Figure 14. Out-of-plane displacement (z direction)

References

Aguiar, R.A.A., Savi, M.A. & Pacheco, P.M.C.L. (2013), "Experimental Investigation of Vibration Reduction Using Shape Memory Alloys", *Journal of Intelligent Material Systems and Structures*, v.24, n.2, pp.247-261.

Auricchio, F., & Taylor, R.L., 1996, "Shape-memory alloys: modeling and numerical simulations of the finite-strain superelastic behavior", *Computational Methods in Applied Mechanics and Engineering*, Vol. 143, pp. 175-194.

Auricchio, F., & Taylor, R.L., 1997, "Shape-memory alloys: macromodelling and numerical simulations of superelastic behavior", *Computational Methods in Applied Mechanics and Engineering*, Vol. 146, pp. 281-312.

Bandeira, E.L., Savi, M.A., Monteiro Jr., P.C.C. & Antoun Netto, T. (2006), "Finite Element Analysis of Shape Memory Alloy Adaptive Trusses with Geometrical Nonlinearities", *Archive of Applied Mechanics*, v.76, n.3-4, pp.133-144.

Bernardini, D.N., & Rega, G., 2005, "Thermomechanical modeling, nonlinear dynamics and chaos in shape memory oscillators", *Mathematical and Computer Modeling of Dynamical Systems*, Vol. 11, No. 3, pp. 291-314.

De Paula, A.S., Savi, M.A., & Lagoudas, D.C., 2011, "Nonlinear dynamics of an SMA large-scale space structure", *Proceedings of the COBEM 2011 - 21th International Congress of Mechanical Engineering*, Natal, Rio Grande de Norte, Brazil.

Hartl, D.J., & Lagoudas, D.C., 2007, "Aerospace applications of shape memory alloys", *Proceedings of the Institution of Mechanical Engineers*, Part G: Journal of Aerospace Engineering, Vol. 221, pp. 535-552.

Lacarbonara, W., Bernardini, D., & Vestroni, F., 2004, "Nonlinear thermomechanical oscillations of shape-memory devices",*International Journal of Solids and Structures*, Vol. 41, No. 5-6, pp. 1209-1234.

La Cava, C.A.P.L., Savi, M.A. & Pacheco, P.M.C.L. (2004), "A Nonlinear Finite Element Method Applied to Shape Memory Bars",*Smart Materials & Structures*, v.13, n.5, pp.1118-1130.

Lagoudas, D.C., 2008, "Shape memory alloys: modeling and engineering applications", Springer.

Lagoudas, D.C., Hartl, J.C., Chemisky, Y., Machado, L.G., & Popov, P., 2012, "Constitutive model for the numerical analysis of phase transformation in polycrystalline shape memory alloys", *International Journal of Plasticity*, Vol. 32-33, pp. 155-183.

Machado, L.G., Lagoudas, D.C., & Savi, M.A., 2009, "Lyapunov exponents estimation for hysteretic systems", *International Journal of Solids and Structures*, Vol. 46, No. 6, pp. 1269-1286.

Machado, L.G., Savi, M.A., & Pacheco, P.M.C.L., 2004, "Bifurcations and crises in a shape memory oscillator", *Shock and Vibration*, Vol. 11, No. 2, pp. 67-80.

Paiva, A. & Savi, M.A. (2006), "An Overview of Constitutive Models for Shape Memory Alloys", *Mathematical Problems in Engineering*, v.2006, Article ID56876, pp.1-30.

Rebelo, N., Walker, N., & Foadian, H., 2001, "Simulation of implantable nitinol stents", *Proceedings of the 2001 Abaqus Users Conference*, pp. 1-14.

Savi, M.A., de Paula, A.S. & Lagoudas, D.C. (2011), "Numerical Investigation of an Adaptive Vibration Absorber Using Shape Memory Alloys", *Journal of Intelligent Material Systems and Structures*, v.22, n.1, pp.67-80.

Savi, M.A., Sa, M.A.N., Paiva, A. & Pacheco, P.M.C.L. (2008), "Tensile-Compressive Asymmetry Influence on the Shape Memory Alloy System Dynamics",*Chaos, Solitons & Fractals*, v.36, n.4, pp.828-842.

Savi, M.A., & Braga, A.M.B., 1993a, "Chaotic vibrations of an oscillator with shape memory", *Journal of Brazilian Society of Mechanical Sciences and Engineering*, Vol. XV, No. 1, pp. 1-20.

Savi, M.A., & Braga, A.M.B., 1993b, "Chaotic response of a shape memory oscillator with internal constrains",

ISSN 2176-5480

Proceedings of the XII Brazilian Congress of Mechanical Engineering, Brasilia, Brazil, pp. 33-36.

Savi, M.A., & Pacheco, P.M.C.L., 2002, "Chaos and hyperchaos in shape memory systems", *International Journal of Bifurcation and Chaos*, Vol. 12, No. 3, pp. 645-657.

7. RESPONSIBILITY NOTICE

The authors are the only responsibles for the printed material included in this paper.